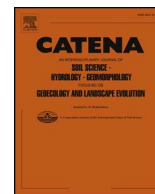




Contents lists available at ScienceDirect

Catena

journal homepage: www.elsevier.com/locate/catena

Micro-characteristics of soil aggregate breakdown under raindrop action

Guanglu Li^{a,b,*}, Yu Fu^b, Baiqiao Li^b, Tenghui Zheng^b, Faqi Wu^a, Guanyun Peng^c, Tiqiao Xiao^c

^a College of Resources and Environment, Northwest A & F University, Yangling 712100, China

^b Institute of Soil and Water Conservation, Northwest A & F University, Yangling 712100, China

^c Shanghai Synchrotron Radiation Facility, Shanghai Institute of Applied Physics, Chinese Academy of Sciences, Shanghai 201204, China

ARTICLE INFO

Keywords:

Raindrop splash
Soil aggregate breakdown
Micro-characteristics
Surface seal
Shape index of aggregate

ABSTRACT

Raindrop splash is considered to be the first step in soil erosion, and it is also a contribution to such erosion. Aggregate breakdown due to raindrop splash causes crusting and soil erosion. In this study, the micro-characteristics of soil aggregate breakdown under the action of three sizes of raindrops were examined using synchrotron-based X-ray micro-computed tomography (SR- μ CT). The results showed that soil aggregate breakdown was related to the size of raindrops, was mainly caused by large raindrops during a rainfall event, and formed an enrichment zone, transition zone, and dense airtight zone of aggregates in the surface soil. The shape index and the amount of aggregate in the splashed soil was higher than in the un-splashed soil, especially for micro-aggregate fragments ($< 25 \mu\text{m}$). We confirm that the existence of large amounts of micro-aggregate fragments surrounding large aggregates in a rainfall event is a principle factor in the formation of soil surface seals and the clogging of pores.

1. Introduction

Raindrop splash is responsible for initiating water erosion because it is the first erosive force to occur during an erosive rainfall event (Sempere et al., 1994; Hudson, 1995; Morgan, 2005; Cuomo et al., 2016). Although the aggregate breakdown caused by raindrop splash can result in pore blockage (Falson et al., 2012) and the formation of a crust (Abu-Hamdeh et al., 2006; Le Bissonais et al., 1989; Warrington et al., 2009; Sajjadi and Mahmoodabadi, 2015) on the surface soil, the fundamental processes associated with the size of raindrops remain unresolved.

Raindrop splash depends on the number, the size and velocity of raindrops impacting the soil surface, which determines the rainfall kinetic energy per unit surface (Ramos et al., 2003; Angulo-Martínez et al., 2012). The detachment of soil aggregates by splash depends not only on the energy of raindrops but also on soil erodibility, which relies on soil physico-chemical characteristics such as infiltration capacity (Fox et al., 2007; Legout et al., 2005a), the nature of soil aggregates (Ma et al., 2014; Huang et al., 2010; Poesen and Torri, 1988), organic matter content (Le Bissonais, 1990) and other factors (Bronick and Lal, 2005). Soil aggregate stability has been used to indicate the resistance of soil to erosive agents and soil quality (Ghadir et al., 2007; Nichols and Toro, 2011; Shainberg et al., 1992; Raine and So, 1993; Jasinska et al., 2006).

Aggregate breakdown and dispersion, which are caused by raindrop

impact, can decrease the soil porosity and the infiltration capacity, and cause surface sealing (Salles et al., 2000; Li et al., 2008; Gregorich et al., 1994; Feller and Beare, 1997). In addition, soil aggregates physically protect organic matter (Field et al., 2006; Li and Pang, 2014; Feller and Beare, 1997), which is important for carbon sequestration. Some researchers have found that when rainfall detachment is the dominant erosion process, the particle size distribution in an eroded soil differs from the original soil (Li and Pang, 2014; Slattery and Burt, 1997). Many studies have also shown that aggregate breakdown due to the raindrop impact is likely to be a main factor affecting particle distribution of sediments (Fu et al., 2016; Fu et al., 2017; Hairsine et al., 1999). Aggregate breakdown produces smaller particle than present on the original soil, which may be displaced and reoriented into a more continuous structure. They clog conducting pores and, consequently, a surface seal is developed (Ramos et al., 2003). The particle distribution of the eroded soil can be influenced by the particle distribution of the original soil, the aggregate breakdown during erosive events and the setting velocity of different size classes of particles (Mahmoodabadi et al., 2014). The particle size distribution of an eroded soil also seems to be dependent on the erosive agent of rainfall and or runoff, flow hydraulic characteristics and slope gradient. Several methods for measuring soil aggregate stability have been developed (Le Bissonais et al., 1989; Le Bissonais, 1990; Pierson and Mulla, 1989; Beare and Bruce, 1993; Loch and Foley, 1994; Amézketa et al., 1996). However, studies on the micro characteristics of soil aggregate breakdown using

* Corresponding author at: College of Resources and Environment, Northwest A & F University, Yangling 712100, China.
E-mail address: guangluli@nwsuaf.edu.cn (G. Li).

<http://dx.doi.org/10.1016/j.catena.2017.10.027>

Received 18 February 2017; Received in revised form 10 October 2017; Accepted 23 October 2017
0341-8162/ © 2017 Elsevier B.V. All rights reserved.

the synchrotron based X-ray micro-computed tomography (SR- μ CT) have not been reported.

In a rainfall event, raindrops occur in various sizes, ranging from large raindrops with a diameter of up to 5 mm to small raindrops with a diameter of < 0.2 mm. The objectives of this research were to evaluate the relationships between rainfall kinetic energies and soil aggregate breakdown by using the synchrotron based X-ray micro-computed tomography (SR- μ CT) and to analyze the morphological characteristic of aggregate breakdown in the splash detachment and transport of aggregate fragments. It may be extremely important for us to reveal decreased infiltration captivity and the formation of crust in the process of soil erosion.

2. Materials and methods

2.1. Soil samples

Soil samples were collected from Yangling, Shanxi Province of China (108°03'30.03"E, 34°18'25.95"N), which is a traditional agricultural planting region. This region has a warm sub-humid continental climate with an annual average temperature of 13 °C and annual precipitation of 550–650 mm, which mainly occurs in July, August and September. The studied soils were formed from erosive loess and are relatively deep. They exhibit a loam or silt-loam texture (according to the USDA particle size classification criteria) (Fu et al., 2016). Major crops grown in this region include maize (*Zea mays* L.) and winter wheat (*Triticum aestivum* Linn.).

Thirty undisturbed soil samples were obtained with a cutting ring (10 cm diameter, 5 cm height) from the top soil layer of croplands (0–5 cm) using the diagonal method at five points. Bulk density was determined with oven-dried at 105 °C until constant mass as described by Blake and Hartge (1986), organic matter by using combustion method, total nitrogen was measured by the semi-micro-Kjeldahl method, soil texture (clay, silt and sand contents) was obtained by the pipette method, and results are shown in Table 1. Aggregate size distribution was determined by wet and dry sieving (Kemper and Rosenau, 1986), and the mass percentage of aggregate in un-splashed soil is also shown in Fig. 1. The obtained results showed that the mean bulk density, soil organic matter, total nitrogen, and total phosphorous for this soil were 1.37 g cm⁻³, 1.46%, 1.04 g kg⁻¹, and 0.62 g kg⁻¹, respectively. The investigated soil was a silty loam with a mean content of silt and clay of 44.07% and 22.67% (according to the USDA particle size classification criteria), respectively.

2.2. Rainfall test

Small raindrops (with a diameter of 2.67 mm), medium raindrops (with a diameter of 3.39 mm) and large raindrops (with a diameter of 5.45 mm) were produced using a raindrop generator (Fig. 2A). The raindrop generator consisted of a cylindrical box with an open top measuring 10 cm in diameter and 10 cm in height. In the floor of the box, 21 syringe needles (US needle of sizes 7 and 16) were installed in a grid of 2 cm. Raindrop size was controlled by changing the needle size and by adjusting the height of the hydraulic head (Fu et al., 2017). The collecting device for the impacted raindrops consisted of stainless steel pan (110 cm diameter). A rainfall duration of 10 min was evaluated for each raindrop diameter, with 5 replications.

For natural rainfall, when the raindrop diameter was greater than or

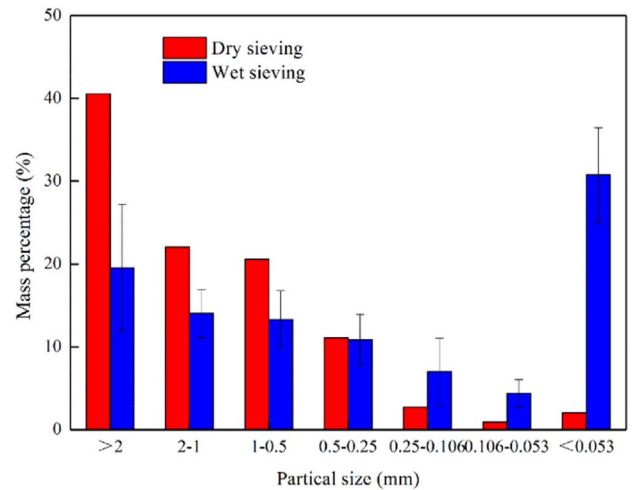


Fig. 1. The fraction percentage for soil aggregate obtained by wet and dry sieving procedure.

equal to 1.9 mm, the terminal velocity of raindrops was calculated by the modified Newton formula; For simulated rainfall, the velocity should be further corrected by Eq. (2) because the raindrops do not reach the terminal velocity (Yao and Chen, 1993). According to the raindrop mass and velocity, the splash energy is calculated by Eq. (3).

$$v_i = (17.20 - 0.844d)\sqrt{0.1d} \quad d \geq 1.9 \quad (1)$$

$$V = v_i \sqrt{1 - e^{-\frac{2g}{v_i^2}H}} \quad (2)$$

$$E_{rs} = \sum_{i=0}^n \frac{1}{2}mV^2 \quad (3)$$

where V is raindrop velocity ($m s^{-1}$), d is the raindrop diameter (mm), v_i is the terminal velocity ($m s^{-1}$), H is the height of falling raindrop (m), E_{rs} is the splash energy of raindrops ($J m^{-2} s^{-1}$), m is the individual raindrop mass (g), $i = 0, \dots, n$ is the number of raindrops, and g is the gravity acceleration ($m s^{-2}$).

The raindrop sizes, splash energies and the main parameters of the simulated raindrops are shown in Table 2. The dry clods (a diameter size of approximately 5 mm) for surface impacted soil (a depth of 0–0.5 cm) and spilled sediment were obtained before and after each rainfall event. A total of 90 dry clods were selected and subjected to CT scanning.

2.3. SR- μ CT scanning

Synchrotron-based X-ray micro-computed tomography (SR- μ CT) (in Shanghai, China) was used to scan the soil clods (with a diameter size of approximately 5 mm) at an energy level of 24 kV and a detection distance of 11 cm, with a pixel size of 3.25 μm . Scanning was performed in continuous scans, and the scanning interval was 0.625 mm (Fig. 2B). After scanning and reorientation, 720 original images (tomo images) were tested for every soil clod (Fig. 2C). The original images were transferred into PITRE (Phase-sensitive X-ray Image Processing and Tomography Reconstruction) software (V3.1) to conduct phase retrieval and slice reconstruction (Chen et al., 2012; Chen et al., 2013). A total of 1500–2000 slices were produced for every soil clod with a pixel

Table 1
Characteristics of the soil at the study site (mean value \pm SD).

Soil type	Bulk density g cm ⁻³	Soil organic matter %	Total nitrogen g kg ⁻¹	Total phosphorus g kg ⁻¹	Sand (%) > 0.02 mm	Silt (%) 0.02–0.002 mm	Clay (%) < 0.002 mm
Loess	1.37 \pm 0.13	1.46 \pm 0.03	1.04 \pm 0.02	0.62 \pm 0.02	33.36 \pm 0.02	44.07 \pm 0.03	22.67 \pm 0.02

Download English Version:

<https://daneshyari.com/en/article/8893773>

Download Persian Version:

<https://daneshyari.com/article/8893773>

[Daneshyari.com](https://daneshyari.com)